Early-Metal Macrocycles as Metalloligands: Synthesis and Structure of Dimeric Zirconocene Dithiolates $Cp_2Zr(\mu\text{-}S(CH_2)_nS)_2ZrCp_2$ (n = 2, 3) and Their Silver Complexes $[(Cp_2Zr(\mu\text{-}S(CH_2)_nS)_2ZrCp_2)Ag]BPh_4$ (n = 2, 3)

Douglas W. Stephan

Department of Chemistry and Biochemistry, University of Windsor, Windsor, Ontario, Canada N9B 3P4

Received November 2, 1990

The reactions of Cp_2ZrMe_2 with the dithiols $HS(CH_2)_nSH$ (n = 2–4) and *o*- and *m*-$HSCH_2C_6H_4CH_2SH$ proceed with evolution of methane, affording the insoluble zirconocene dithiolate derivatives. In the case of $HS(CH_2)_nSH$, where n = 2 and 3, the products can also be synthesized via reaction of Cp_2ZrMe_2 or $[Cp_2ZrHCl]_n$ with $HS(CH_2)_nSSiMe_3$ (n = 2, 3). Crystallographic studies of two of these products show that there are bimetallic compounds. The compound $Cp_2Zr(\mu\text{-}SCH_2CH_2S)_2ZrCp_2$ (**1a**) crystallizes in the space group $P2_1$ with a = 8.072 (1) Å, b = 8.309 (1) Å, c = 18.066 (2) Å, β = 100.97 (1)°, Z = 2, and V = 1189.5 (3) Å^3. This species is best described as a twisted macrocycle in which two of the four sulfur atoms bridge the two Zr centers. The molecule $Cp_2Zr(\mu\text{-}SCH_2CH_2CH_2S)_2ZrCp_2$ (**1b**) crystallizes in the space group *Pbca* with a = 25.772 (2) Å, b = 15.607 (2) Å, c = 13.008 (1) Å, Z = 8, and V = 5229 (1) Å^3. In contrast to **1a** this species is a true macrocycle that incorporates two zirconocene dithiolate moieties in a 12-membered ring with a Zr(1)···Zr(2) separation of 7.570 (1) Å. Molecules **1a** and **1b** are shown to act as metalloligands, as each reacts with $AgBPh_4$ to yield the 1:1 silver–ligand derivatives. Crystallographic studies confirm that both **1a** and **1b** act as macrocyclic metalloligands, presenting a four sulfur coordination sphere to the encapsulated silver ion. The complex $[(Cp_2Zr(\mu\text{-}SCH_2CH_2S)_2ZrCp_2)Ag]BPh_4$ (**2a**) crystallizes in the space group $P2_1/n$ with a = 8.718 (3) Å, b = 31.492 (9) Å, c = 15.847 (3) Å, β = 92.21 (2)°, Z = 4, and V = 4348 (2) Å^3. Molecule $[(Cp_2Zr(\mu\text{-}SCH_2CH_2CH_2S)_2ZrCp_2)Ag]BPh_4$ (**2b**) crystallizes in the space group $P\bar{1}$ with a = 11.242 (4) Å, b = 12.790 (7) Å, c = 18.270 (10) Å, α = 112.33 (4)°, β = 111.23 (4)°, γ = 81.81 (4)°, Z = 2, and V = 2265 (5) Å^3. The results of these studies are discussed, and the implications of the data are considered.

Introduction

Complexes containing both an early, oxophilic metal and a late, electron-rich metal center have been the subject of numerous recent reports.[1] The motivation for this interest stems, in part, from the perspective of synthetic methodology development and, in part, from the potential for new reactivity patterns arising from the derived early–late heterobimetallics (ELHB). Precedent for the later view has been established in the heterogeneous catalysis literature, where, indeed, unique behavior is derived from late-metal catalysts dispersed on early-metal supports.[2,3] Such strong metal-support interactions (SMSI) are not well understood but have been attributed to both electronic communication between the disparate metal centers and cooperative activation of substrates by the different metal centers.[2,3]

In the pursuit of synthetic routes to homogeneous complexes that incorporate widely divergent metal types a number of approaches have been undertaken. We are among those who have adopted the early-metal "metalloligand" approach.[1] In this method, early-metal complexes are functionalized to act as ligands for late metals. For example, we have employed early-metal phosphides,[4–10] thiolates,[11–13] and pendent chelating metalloligands[14–16] in the synthesis of ELHB species. In the case of thiolate-bridged ELHB complexes, we have previously described a variety of Ti/Cu,[11] Ti/Ni,[12] and V/Cu[13] species in which close proximity of disparate metal centers is achieved. However, these complexes prove to be generally unstable and difficult to prepare and/or isolate. In contrast, macrocyclic ligands containing sulfur donors have been shown to stabilize a variety of metal complexes.[17] The demonstrated stability and ability of macrocycles to bind transition metals in a variety of oxidation states prompted our efforts to apply this principle to the synthesis of ELHB complexes. We have previously shown that the reaction of Cp_2ZrMe_2 with simple diols led to the formation of macrocyclic zirconocene dialkoxides (e.g. A and B).[18] Previous reports in the literature[19,20] have described early metallocene derivatives of dithiols as simple mononuclear chelate complexes. We report herein, the synthesis and structures of the first bimetallic, macrocyclic, zirconocene dithiolate complexes. Further, we describe their use as metalloligands for the complexation of silver. Structural studies of two such derivatives are presented. The results of these studies are discussed, and the implications are considered. Some of these results have been previously communicated.[21]

(1) Stephan, D. W. *Coord. Chem. Rev.* **1989**, *95*, 42.
(2) *Metal-Support Interactions in Catalysis, Sintering, and Redispersion*; Stevenson, S. A., Dumesic, J. A., Baker, R. T. K., Ruckenstein, E., Eds.; Van Nostrand Reinhold Co.: New York, 1987.
(3) *Strong Metal-Support Interactions*; Baker, R. T. K., Tauster, S. J., Dumesic, J. A., Eds.; American Chemical Society: Washington, DC, 1986.
(4) Gelmini, L.; Stephan, D. W. *Inorg. Chim. Acta* **1986**, *111*, L17.
(5) Gelmini, L.; Matassa, L. C.; Stephan, D. W. *Inorg. Chem.* **1985**, *24*, 2585.
(6) Gelmini, L.; Stephan, D. W. *Inorg. Chem.* **1986**, *25*, 1222.
(7) Gelmini, L.; Stephan, D. W. *Organometallics* **1988**, *7*, 849.
(8) Zheng, P. Y.; Nadasdi, T. T.; Stephan, D. W. *Organometallics* **1989**, *8*, 1393.
(9) Dick, D. G.; Stephan, D. W. *Organometallics* **1990**, *9*, 1910.
(10) Dick, D. G.; Stephan, D. W. Unpublished results.
(11) Wark, T. A.; Stephan, D. W. *Inorg. Chem.* **1987**, *26*, 363.
(12) Wark, T. A.; Stephan, D. W. *Organometallics* **1989**, *8*, 2836.
(13) Wark, T. A.; Stephan, D. W. *Inorg. Chem.* **1990**, *29*, 1731.
(14) White, G. S.; Stephan, D. W. *Inorg. Chem.* **1985**, *24*, 1499.
(15) White, G. S.; Stephan, D. W. *Organometallics* **1987**, *6*, 2169.
(16) White, G. S.; Stephan, D. W. *Organometallics* **1988**, *7*, 903.
(17) Blake, A. J.; Schröder, M. *Adv. Inorg. Chem.* **1990**, *35*, 2.
(18) Stephan, D. W. *Organometallics* **1990**, *9*, 2718.
(19) Chaudari, M. A.; Stone, F. G. A. *J. Chem. Soc. A* **1966**, 838.
(20) Meunier, P.; Gautheron, B.; Mazouz, A. *J. Chem. Soc., Chem. Commun.* **1988**, 424.

0276-7333/91/2310-2037$02.50/0

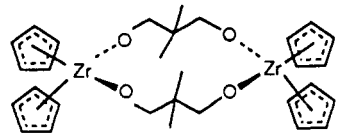

A

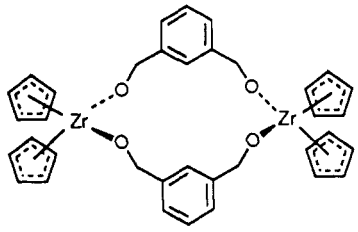

B

Experimental Section

General Data. All preparations were done under an atmosphere of dry, O_2-free N_2 employing a Vacuum Atmospheres inert-atmosphere glovebox. Solvents were reagent grade, distilled from the appropriate drying agents under N_2 and degassed by the freeze–thaw method at least three times prior to use. ^1H NMR spectra were recorded on Bruker AC-300 spectrometer operating at 300 MHz. Trace amounts of protonated solvents were used as reference, and chemical shifts are reported relative to $SiMe_4$. Combustion analyses were performed by Galbraith Laboratories Inc., Knoxville, TN, and Schwarzkopf Laboratories, Woodside, NY. Cp_2ZrCl_2, MeLi, 1,2-ethanedithiol, 1,3-propanedithiol, 1,4-butanedithiol, *o*-xylenedithiol, and trimethylsilyl chloride were purchased from the Aldrich Chemical Co. $AgBPh_4$,[22] Cp_2ZrMe_2,[23] and *m*-xylenedithiol[24] were prepared by the literature method.

Synthesis of $HSCH_2CH_2SSiMe_3$. To a solution of 1,2-propanedithiol (9.4 g, 0.1 mol) in ether at −78 °C was added 40 mL of *n*-BuLi in hexane (2.5 M). The mixture was stirred for 2 h. Me_3SiCl (7.8 m, 0.1 mol) was added and the mixture stirred overnight as it gradually warmed to 25 °C. The solution was filtered under an inert atmosphere and the solvent removed under vacuum. The product was distilled as a colorless liquid at 49–50 °C (0.01 Torr). Yield: 5.85 g (35%). ^1H NMR (δ, 298 K, $CDCl_3$): HS, 1.65 (s, 1 H); CH_2, 2.62 (s, 4 H); CH_3, 0.24 (s, 9 H). $^{13}C\{^1H\}$ NMR (δ, 298 K, $CDCl_3$): CH_2, 30.22, 27.28; CH_3, 0.85.

Synthesis of $HSCH_2CH_2CH_2SSiMe_3$. This compound was prepared as $HSCH_2CH_2SSiMe_3$ by employing 5.40 g of 1,3-propanedithiol, 20 mL of *n*-BuLi in hexane (2.5 M), and 5.45 g of Me_3SiCl. The yield of $HSCH_2CH_2CH_2SSiMe_3$ was 4.3 g (48%); bp 68–70 °C (0.01 Torr). ^1H NMR (δ, 298 K, $CDCl_3$): HS, 1.28 (t, 1 H), $|J_{H-H}|$ = 7.3 Hz; CH_2, 1.81 (q, 2 H), $|J_{H-H}|$ = 3.9 Hz, 2.5 (m, 4 H); CH_3, 0.24 (s, 9 H). $^{13}C\{^1H\}$ NMR (δ, 298 K, $CDCl_3$): CH_2, 36.45, 24.64, 23.28; CH_3, 1.03.

Synthesis of $Cp_2Zr(\mu\text{-SRS})_2ZrCp_2$ (R = $(CH_2)_2$ (1a), $(CH_2)_3$ (1b), $(CH_2)_4$ (1c), *o*-$CH_2C_6H_4CH_2$ (1d), *m*-$CH_2C_6H_4CH_2$ (1e)). Each of these compounds were prepared in a similar manner, and thus, only one such preparation is described.

Method i from Cp_2ZrMe_2 and Dithiol. To a solution of Cp_2ZrMe_2 (0.100 g, 0.342 mmol) in 3 mL of THF was added 1,3-propanedithiol (0.037 g, 0.342 mmol). The evolution of methane was observed immediately, and the bubbling slowed but continued for about 1 h. At this point, the solution became yellow in color. The solution was allowed to stand for several hours. About 2 mL of hexane was added, and the solution was allowed to stand overnight. Yellow crystals of the product **1b** precipitated from solution. Separation was achieved by decantation of the mother liquor. Crystalline product was also obtained for **1a** and **1c**, while clean, yellow powders were obtained for **1d** and **1e**. Data for **1a** are as follows. Yield: 40%. ^1H NMR (δ, 298 K, $CDCl_3$): C_5H_5, 5.96 (s, 20 H); CH_2, 3.04 (t, 4 H), $|J_{H-H}|$ = 5.5 Hz, 2.72 (t, 4 H). $^{13}C\{^1H\}$ NMR (δ, 298 K, $CDCl_3$): C_5H_5, 111.44; CH_2, 40.40, 38.65. Anal. Calcd for $C_{24}H_{28}S_4Zr_2$: C, 45.96; H, 4.50. Found: C, 45.17; H, 4.41. Data for **1b** are as follows. Yield: 44%. ^1H NMR (δ, 298 K, $CDCl_3$): C_5H_5, 6.17 (s, 20 H); CH_2, 2.98 (t, 8 H), $|J_{H-H}|$ = 6.8 Hz, 1.95 (q, 4 H). $^{13}C\{^1H\}$ NMR (δ, 298 K, $CDCl_3$): C_5H_5, 110.55; CH_2, 36.78, 35.75. Anal. Calcd for $C_{26}H_{32}S_4Zr_2$: C, 47.66; H, 4.92. Found: C, 46.31; H, 4.73. Data for **1c** are as follows. Yield: 55% (by NMR). ^1H NMR (δ, 298 K, $CDCl_3$): C_5H_5, 6.17 (s, 20 H); CH_2, 2.92 (m, 8 H), 1.61 (m, 8 H). Anal. Calcd for $C_{28}H_{36}S_4Zr_2$: C, 49.22; H, 5.31. Found: C, 48.19; H, 5.12. Data for **1d** are as follows. Yield: 42% (by NMR). ^1H NMR (δ, 298 K, $CDCl_3$): C_6H_4, 7.2 (m, 8 H); C_5H_5, 6.29 (s, 20 H); CH_2, 4.19 (s, 8 H). Anal. Calcd for $C_{36}H_{36}S_4Zr_2$: C, 55.48; H, 4.66. Found: C, 55.19; H, 4.75. Data for **1e** are as follows. Yield: 44% (by NMR). ^1H NMR (δ, 298 K, $CDCl_3$): C_6H_4, 7.2 (m, 8 H); C_5H_5, 6.27 (s, 20 H); CH_2, 4.12 (s, 8 H). Anal. Calcd for $C_{36}H_{36}S_4Zr_2$: C, 55.48; H, 4.66. Found: C, 54.01; H, 4.71.

Method ii from Cp_2ZrMe_2 and $HS(CH_2)_nSSiMe_3$ (*n* = 2, 3). To a solution of Cp_2ZrMe_2 (0.100 g, 0.342 mmol) in 3 mL of THF was added $HSCH_2CH_2CH_2SSiMe_3$ (0.074 g, 0.342 mmol). The slow evolution of methane was observed. The solution became yellow in color over the next 24-h period. About 2 mL of hexane was added, and the solution was allowed to stand overnight. Yellow crystals of the product **1b** precipitated from solution. Separation was achieved by decantation of the mother liquor. Yields (by NMR): **1a**, 67%; **1b**, 60%.

Method iii from $[Cp_2ZrHCl]_n$ and $HS(CH_2)_nSSiMe_3$ (*n* = 2, 3). To a solution of $[Cp_2ZrCl]_n$ (0.100 g, 0.342 mmol) in 3 mL of THF was added $HSCH_2CH_2CH_2SSiMe_3$ (0.072 g, 0.342 mmol). The rapid evolution of methane was observed, and the solution became yellow within 10 min. The solution was allowed to stand for 24 h. About 2 mL of hexane was added, and the solution was allowed to stand overnight. Yellow crystals of the product **1b** precipitated from solution. Separation was achieved by decantation of the mother liquor. Yields (by NMR): **1a**, 50%; **1b**, 55%.

Synthesis of $[(Cp_2Zr(\mu\text{-SRS})_2ZrCp_2)Ag]BPh_4$ (R = $(CH_2)_2$ (2a), $(CH_2)_3$ (2b)). These complexes were prepared in a similar manner; thus, only one typical preparation is described. To a suspension of **1a** (0.100 g, 0.160 mmol) in CH_2Cl_2 (2 mL) was added $AgBPh_4$ (0.068 , 0.160 mmol) in CH_2Cl_2. The solution gradually became yellow as the solid **1a** dissolved. After the reaction was allowed to stand for several hours, the solution was filtered and about 2 mL of THF and 2 mL of hexane was added. On standing overnight, large blocklike crystals of **2a** formed. Separation of the product from the mother liquor was achieved by decantation. Data for **2a** are as follows. Yield (isolated): 30%. ^1H NMR (δ, 298 K, CD_2Cl_2): C_6H_5, 7.35 (m, 8 H), 7.05 (t, 8 H), 6.89 (t, 4 H), $|J_{H-H}|$ = 7.2 Hz; C_5H_5, 6.21 (s, 20 H); CH_2, 3.94 (d, 4 H), 3.07 (d, 4 H), $|J_{H-H}|$ = 10.5 Hz. Anal. Calcd for $C_{48}H_{48}AgBS_4Zr_2$: C, 62.93; H, 7.54. Found: C, 62.50; H, 7.50. Data for **2b** are as follows. Yield (isolated): 45%. ^1H NMR (δ, 298 K, CD_2Cl_2): C_6H_5, 7.32 (m, 8 H), 7.04 (t, 8 H), 6.89 (t, 4 H), $|J_{H-H}|$ = 7.1 Hz; C_5H_5, 6.28 (s, 20 H); CH_2, 3.37 (br m, 4 H), 3.14 (br m, 4 H), 2.07 (q, 4 H), $|J_{H-H}|$ = 5.9 Hz. $^{13}C\{^1H\}$ NMR (δ, 298 K, CD_2Cl_2): C_6H_5, 136.3, 126.0, 122.1; C_5H_5, 112.4; CH_2, 37.5, 31.8. Anal. Calcd for $C_{50}H_{52}AgBS_4Zr_2$: C, 62.93; H, 7.54. Found: C, 62.50; H, 7.50.

X-ray Data Collection and Reduction. X-ray-quality crystals of **1a**, **1b**, **2a**, and **2b** were obtained directly from the preparations as described above. The crystals were manipulated and mounted in capillaries in a glovebox, thus maintaining a dry, O_2-free environment for each crystal. Diffraction experiments were performed either on a four-circle Syntex $P2_1$ diffractometer or on a Rigaku AFC6-S four-circle diffractometer with graphite-monochromatized Mo Kα radiation. For **1b** and **2b**, the initial orientation matrices were obtained from 15 machine-centered reflections selected from rotation photographs. In the case of **1a** and **2a**, the initial orientation matrices were obtained from 20 reflections located by an autosearch routine. These data were used to determine the crystal systems. Partial rotation photographs around each axis were consistent with orthorhombic and triclinic crystal systems for **1b** and **2b**, respectively. Ultimately, 56 and 39 reflections (20° < 2θ < 25°) were used to obtain the final lattice parameters and the orientation matrices for **1b** and **2b**, respectively. For **1a** and **2a**, the symmetries of the respective lattices were found to be consistent with monoclinic crystal systems and in each case 25 reflections (20° < 2θ < 37°) were used

(21) Stephan, D. W. *J. Chem. Soc., Chem. Commun.* **1991**, 129.
(22) Jordan, R. F.; Echols, S. F. *Inorg. Chem.* **1987**, *26*, 383.
(23) Hunter, W. E.; Hrncir, D. C.; Vann Bynum, R.; Penttila, R. A.; Atwood, J. L. *Organometallics* **1983**, *2*, 750.
(24) Mayerle, J. J.; Denmark, S. E.; DePamphilis, B. V.; Ibers, J. A.; Holm, R. H. *J. Am. Chem. Soc.* **1975**, *97*, 1032.

Table I. Crystallographic Parameters

	molecule **1a**	molecule **1b**	molecule **2a**	molecule **2b**
formula	$C_{24}H_{28}S_4Zr_2$	$C_{26}H_{32}S_4Zr_2$	$C_{48}H_{48}AgBS_4Zr_2$	$C_{50}H_{52}AgBS_4Zr_2$
cryst color, form	yellow blocks	yellow blocks	colorless blocks	colorless blocks
a, Å	8.072 (1)	25.772 (2)	8.718 (3)	11.242 (4)
b, Å	8.309 (1)	15.607 (2)	31.492 (9)	12.790 (7)
c, Å	18.066 (2)	13.008 (1)	15.847 (3)	18.270 (10)
α, deg				112.33 (4)
β, deg	100.97 (1)		92.21 (2)	111.23 (4)
γ, deg				81.81 (4)
cryst syst	monoclinic	orthorhombic	monoclinic	triclinic
space group	$P2_1$ (No. 4)	$Pbca$ (No. 61)	$P2_1/n$ (No. 14)	$P\bar{1}$ (No. 2)
V, Å^3	1189.5 (3)	3229 (1)	4348 (2)	2265 (5)
density calcd, g cm^{-1}	1.75	1.66	1.61	1.59
Z	2	8	4	2
cryst dimens, mm	0.30 × 0.35 × 0.45	0.43 × 0.38 × 0.44	0.40 × 0.35 × 0.45	0.45 × 0.32 × 0.44
abs coeff μ, cm^{-1}	12.11	11.05	11.22	10.79
radiation λ, Å	Mo Kα (0.71069)	Mo Kα (0.71069)	Mo Kα (0.71069)	Mo Kα (0.71069)
temp, °C	24	24	24	24
scan speed, deg/min	32.0 ($\theta/2\theta$)	2.0–8.0 ($\theta/2\theta$)	32.0 ($\theta/2\theta$)	2.0–5.0 ($\theta/2\theta$)
scan range, deg	1.0 below Kα_1	1.0 below Kα_1	1.0 below Kα_1	1.0 below Kα_1
	1.0 above Kα_2	1.0 above Kα_2	1.0 above Kα_2	1.0 above Kα_2
bkgd/scan time ratio	0.5	0.5	0.5	0.5
no. of data collcd	2423	3859	8564	5946
2θ range, deg	4.5–50	4.5–45.0	4.5–50	4.5–45.0
index range	$h,k,\pm l$	h,k,l	$h,k,\pm l$	$\pm h,\pm k,+l$
no. of data with $F_o^2 > 3\sigma(F_o^2)$	1449	2674	3345	2933
no. of variables	112	289	380	398
R, %	6.94	3.65	7.3	6.9
R_w, %	7.73	4.96	8.2	7.9
largest Δ/σ in final least-squares cycle	0.07	0.004	0.014	0.0001
goodness of fit	2.478	1.567	2.067	1.954

to determine the final cell constants. Machine parameters, crystal data, and data collection parameters are summarized in Table I. The observed extinctions and/or structure refinements confirmed the space groups $P2_1$, $Pbca$, $P2_1/n$, and $P\bar{1}$ for **1a**, **1b**, **2a**, and **2b**, respectively. The data sets were collected in one shell (4.5° < 2θ < 45.0°), and three standard reflections were recorded every 197 reflections for **1b** and **2b**. For **1a** and **2a**, standards were measured every 150 reflections. The intensities of the standards showed no statistically significant change over the duration of the data collection. The data were processed by using the TEXSAN software program package on a VAX workstation 3520 located in the Department of Chemistry and Biochemistry at the University of Windsor. The reflections with $F_o^2 > 3\sigma(F_o^2)$ were used in each of the refinements.

Structure Solution and Refinement. Non-hydrogen atomic scattering factors were taken from the literature tabultions.[25,26] The heavy-atom positions for each structure were determined by using direct methods employing the Mithril option of the TEXSAN package. The remaining non-hydrogen atoms were located from successive difference Fourier map calculations. The refinements were carried out by using full-matrix, least-squares techniques on F, minimizing the function $w(|F_o| - |F_c|)^2$, where the weight, w, is defined as $1/\sigma^2(F_o)$ and F_o and F_c are the observed and calculated structure factor amplitudes. In the refinement of **1a**, difference Fourier calculations revealed a disorder of the bridging sulfur atom positions. Refinement of the site occupancies showed that the disorder was best modeled by a 60:40 occupancy of the two positions. This disorder led to poor agreement of the chemically equivalent bond distances in the ethylene chain of the dithiolate ligands. Similar discrepancies have been observed for other species containing disordered dithiolate fragments. In the final refinement it was necessary to constrain the geometry of the cyclopentadienyl rings to that of regular pentagons and only the Zr atoms and S(1) and S(4) could be refined anisotropically. The initial model was confirmed to be the correct enantiomorph by inversion and refinement. In the case of **1b**, the refinement was much better; however, here too, one of the central methylene carbons was disordered. This was modeled by employing two locations of the single carbon atoms with site occupancies of 0.7 and 0.3. In the final cycles of refinement all the remaining non-hydrogen atoms in **1b** were refined as individual anisotropic atoms. In the final cycles of refinement for **2a** and **2b**, all the non-hydrogen atoms of the cation were refined anisotropically. In these cases, the atoms of the anion were refined isotropically. In all cases, hydrogen atom positions were calculated by assuming a C–H bond length of 0.95 Å. Hydrogen atom temperture factors were fixed at 1.10 times the isotropic temperature factor of the carbon atom to which they are bonded. In all cases the hydrogen atom contributions were calculated but not refined. The final refinement data are given in Table I. The largest peaks in the final difference Fourier map calculation showed residual electron densities of no chemical significance. The following data are tabulated: positional parameters (Table II) and selected bond distances and angles (Table III). Thermal parameters, hydrogen atom parameters, bond distances and angles associated the tetraphenylborate anions, and values of $10F_o$ and $10F_c$ have been deposited as supplementary material.

Results and Discussion

We have previously described the formation of macrocyclic zirconocene dialkoxides from the reactions of Cp_2ZrMe_2 with diols.[18] Similar reactions of metal alkyls with acidic proton sources have been known for some time to result in metal–carbon bond cleavage and formation of a metal–heteroatom bond.[27] In a similar vein, reaction of Cp_2ZrMe_2 with several dithiols including $HS(CH_2)_nSH$ (n = 2–4) and o- and m-$HSCH_2C_6H_4CH_2SH$ proceed with the rapid liberation of methane. The resulting zirconium dithiolate species **1** either crystallize on standing or precipitate as clean, yellow powders. The isolated solids are not soluble in THF, acetone, benzene, or CH_2Cl_2. ^1H NMR spectra in $CDCl_3$ solution and combustion analyses are consistent with the empirical formulations Cp_2Zr(dithiolate). The poor solubility in common organic solvents is not typical of mononuclear metallocene dithiolates,[12] suggesting that the present complexes are higher oligomers.

(25) (a) Cromer, D. T.; Mann, J. B. *Acta Crystallogr., Sect. A: Cryst. Phys., Diffr., Theor. Gen. Crystallogr.* **1968**, *A24*, 324. (b) *Ibid.* **1968**, *A24*, 390.

(26) Cromer, D. T.; Waber, J. T. *International Tables for X-ray Crystallography*; Kynoch Press: Birmingham, England, 1974.

(27) Babaian, E. A.; Hrncir, D. C.; Bott, S. G.; Atwood, J. L. *Inorg. Chem.* **1986**, *25*, 4818.

Table II. Positional Parameters for Molecules 1a–2b

atom	x	y	z	atom	x	y	z
			Molecule 1a				
Zr(1)	0.8311 (3)	0.2498	0.6403 (1)	C(5)	0.523 (2)	0.326 (3)	0.601 (1)
Zr(2)	0.6838 (3)	0.1197 (3)	0.8629 (1)	C(6)	0.927 (2)	0.085 (2)	0.5396 (8)
S(1)	1.064 (2)	0.460 (2)	0.6781 (8)	C(7)	1.070 (2)	0.130 (2)	0.592 (1)
S(2A)	0.614 (2)	0.082 (2)	0.7132 (8)	C(8)	1.066 (2)	0.050 (2)	0.6598 (8)
S(2B)	0.715 (2)	0.021 (2)	0.7225 (8)	C(9)	0.920 (2)	−0.045 (2)	0.6491 (9)
S(3A)	0.824 (1)	0.317 (1)	0.7791 (5)	C(10)	0.834 (2)	−0.023 (2)	0.575 (1)
S(3B)	0.910 (2)	0.274 (2)	0.7868 (8)	C(11)	0.389 (2)	0.253 (2)	0.8634 (9)
S(4)	0.4272 (8)	−0.086 (1)	0.8226 (4)	C(12)	0.507 (3)	0.374 (2)	0.860 (1)
C(21)	1.034 (5)	0.553 (5)	0.755 (2)	C(13)	0.623 (2)	0.374 (2)	0.929 (1)
C(22)	1.006 (4)	0.469 (4)	0.823 (2)	C(14)	0.575 (2)	0.252 (3)	0.9742 (9)
C(23)	0.521 (3)	−0.098 (3)	0.684 (1)	C(15)	0.431 (2)	0.177 (2)	0.934 (1)
C(24)	0.494 (2)	−0.211 (3)	0.746 (1)	C(16)	0.886 (2)	0.072 (2)	0.9876 (8)
C(1)	0.603 (3)	0.472 (2)	0.626 (1)	C(17)	0.992 (2)	0.081 (2)	0.935 (1)
C(2)	0.712 (2)	0.511 (2)	0.576 (1)	C(18)	0.953 (2)	−0.048 (2)	0.8845 (9)
C(3)	0.699 (2)	0.390 (3)	0.522 (1)	C(19)	0.824 (2)	−0.138 (2)	0.907 (1)
C(4)	0.582 (2)	0.276 (2)	0.537 (1)	C(20)	0.782 (2)	−0.063 (2)	0.970 (1)
			Molecule 1b				
Zr(1)	0.51102 (2)	−0.13904 (3)	−0.24118 (4)	C(12)	0.7746 (2)	0.0225 (4)	−0.2757 (5)
Zr(2)	0.74400 (2)	0.15129 (3)	−0.17580 (4)	C(13)	0.8053 (2)	0.0265 (4)	−0.1880 (5)
S(1)	00.59698 (6)	−0.1523 (1)	−0.3312 (1)	C(14)	0.8356 (2)	0.1008 (4)	−0.1915 (5)
S(2)	0.52728 (7)	−0.0081 (1)	−0.1379 (1)	C(15)	0.8239 (2)	0.1430 (4)	−0.2839 (5)
S(3)	0.66844 (6)	0.1785 (1)	−0.2941 (1)	C(16)	0.7889 (3)	0.2538 (5)	−0.0580 (6)
S(4)	0.70689 (6)	0.0385 (1)	−0.0610 (1)	C(17)	0.7812 (3)	0.2983 (4)	−0.1494 (7)
C(1)	0.4386 (3)	−0.0384 (4)	−0.2864 (6)	C(18)	0.7283 (3)	0.3087 (4)	−0.1628 (6)
C(2)	0.4757 (3)	−0.0293 (4)	−0.3629 (5)	C(19)	0.7029 (3)	0.2728 (4)	−0.0797 (7)
C(3)	0.4784 (3)	−0.1046 (4)	−0.4180 (5)	C(20)	0.7402 (3)	0.2397 (5)	−0.0144 (6)
C(4)	0.4432 (3)	−0.1617 (4)	−0.3741 (5)	C(21)	0.6145 (3)	−0.0569 (4)	−0.4025 (5)
C(5)	0.4184 (2)	−0.1204 (5)	−0.2937 (5)	C(22)	0.6308 (3)	0.0163 (4)	−0.3273 (5)
C(6)	0.4856 (3)	−0.2913 (4)	−0.2041 (6)	C(23)	0.6535 (3)	0.0920 (5)	−0.3809 (6)
C(7)	0.4681 (3)	−0.2418 (4)	−0.1220 (5)	C(24)	0.6510 (3)	0.0769 (5)	0.0107 (7)
C(8)	0.5111 (3)	−0.2109 (5)	−0.0677 (5)	C(25A)	0.6037 (3)	0.0746 (5)	−0.0379 (6)
C(9)	0.5552 (3)	−0.2406 (5)	−0.1193 (6)	C(25B)	0.6079 (7)	0.022 (1)	0.026 (1)
C(10)	0.5396 (3)	−0.2894 (4)	−0.2028 (7)	C(26)	0.5843 (3)	−0.0238 (6)	−0.0577 (6)
C(11)	0.7868 (2)	0.0947 (4)	−0.3359 (5)				
			Molecule 2a				
Ag(1)	0.1008 (2)	0.09851 (5)	0.3974 (1)	C(22)	0.405 (2)	0.1145 (6)	0.511 (1)
Zr(1)	0.1732 (2)	0.02190 (6)	0.2885 (1)	C(23)	−0.206 (2)	0.0843 (6)	0.285 (1)
Zr(2)	0.0441 (2)	0.18378 (5)	0.4831 (1)	C(24)	−0.229 (2)	0.1254 (6)	0.333 (1)
S(1)	0.3622 (6)	0.0786 (2)	0.3487 (3)	C(31)	0.209 (2)	0.1001 (5)	0.876 (1)
S(2)	−0.0897 (5)	0.0448 (1)	0.3453 (3)	C(32)	0.217 (2)	0.0885 (6)	0.791 (1)
S(3)	−0.0576 (6)	0.1576 (1)	0.3385 (3)	C(33)	0.272 (2)	0.0502 (6)	0.765 (1)
S(4)	0.2035 (6)	0.1189 (2)	0.5410 (3)	C(34)	0.321 (2)	0.0200 (6)	0.825 (1)
C(1)	0.145 (3)	0.0730 (5)	0.167 (1)	C(35)	0.314 (2)	0.0290 (6)	0.909 (1)
C(2)	0.039 (2)	0.0399 (6)	0.150 (1)	C(36)	0.253 (2)	0.0685 (6)	0.932 (1)
C(3)	0.121 (2)	0.0015 (5)	0.138 (1)	C(41)	0.191 (2)	0.1599 (6)	1.000 (1)
C(4)	0.274 (2)	0.0129 (5)	0.147 (1)	C(42)	0.344 (2)	0.1548 (6)	1.030 (1)
C(5)	0.290 (2)	0.0517 (6)	0.163 (1)	C(43)	0.395 (2)	0.1679 (6)	1.110 (1)
C(6)	0.338 (2)	−0.0243 (6)	0.382 (1)	C(44)	0.293 (3)	0.1860 (7)	1.164 (1)
C(7)	0.198 (3)	−0.0194 (7)	0.424 (1)	C(45)	0.141 (2)	0.1895 (7)	1.138 (1)
C(8)	0.087 (3)	−0.0386 (8)	0.374 (2)	C(46)	0.094 (2)	0.1774 (6)	1.058 (1)
C(9)	0.153 (3)	−0.0569 (7)	0.305 (1)	C(51)	−0.055 (2)	0.1351 (6)	0.899 (1)
C(10)	0.312 (3)	−0.0478 (7)	0.308 (1)	C(52)	−0.120 (2)	0.1091 (7)	0.954 (1)
C(11)	−0.180 (2)	0.1478 (7)	0.548 (1)	C(53)	−0.275 (2)	0.0961 (7)	0.946 (1)
C(12)	−0.238 (2)	0.1853 (7)	0.509 (1)	C(54)	−0.361 (2)	0.1115 (7)	0.881 (1)
C(13)	−0.171 (2)	0.2198 (6)	0.549 (1)	C(55)	−0.301 (3)	0.1407 (7)	0.826 (1)
C(14)	−0.077 (2)	0.2044 (9)	0.615 (1)	C(56)	−0.150 (2)	0.1502 (6)	0.834 (1)
C(15)	−0.081 (3)	0.1613 (7)	0.616 (1)	C(61)	0.182 (2)	0.1855 (6)	0.845 (1)
C(16)	0.101 (2)	0.2575 (7)	0.440 (1)	C(62)	0.105 (2)	0.2224 (6)	0.852 (1)
C(17)	0.190 (3)	0.2503 (8)	0.513 (1)	C(63)	0.138 (2)	0.2591 (6)	0.802 (1)
C(18)	0.297 (3)	0.2200 (7)	0.497 (1)	C(64)	0.255 (2)	0.2570 (7)	0.747 (1)
C(19)	0.276 (2)	0.2079 (6)	0.410 (1)	C(65)	0.339 (2)	0.2216 (7)	0.742 (1)
C(20)	0.156 (2)	0.2320 (6)	0.375 (1)	C(66)	0.303 (2)	0.1858 (6)	0.789 (1)
C(21)	0.435 (2)	0.0727 (6)	0.459 (1)	B(1)	0.135 (2)	0.1454 (6)	0.906 (1)
			Molecule 2b				
Ag(1)	0.4701 (1)	0.2061 (1)	0.2856 (1)	C(4)	0.763 (2)	0.335 (3)	0.602 (2)
Zr(1)	0.6476 (2)	0.1846 (1)	0.4702 (1)	C(5)	0.693 (4)	0.392 (2)	0.551 (2)
Zr(2)	0.2931 (2)	0.2361 (1)	0.1073 (1)	C(6)	0.644 (2)	−0.023 (2)	0.447 (2)
S(1)	0.7060 (4)	0.2584 (4)	0.3762 (3)	C(7)	0.702 (2)	−0.015 (1)	0.393 (1)
S(2)	0.4176 (5)	0.1220 (4)	0.3829 (3)	C(8)	0.818 (2)	0.042 (2)	0.444 (2)
S(3)	0.5178 (4)	0.1531 (4)	0.1434 (3)	C(9)	0.830 (2)	0.071 (2)	0.527 (1)
S(4)	0.2378 (5)	0.2814 (4)	0.2403 (3)	C(10)	0.721 (2)	0.031 (2)	0.527 (1)
C(1)	0.568 (3)	0.379 (2)	0.538 (2)	C(11)	0.235 (3)	0.034 (2)	0.051 (2)
C(2)	0.560 (3)	0.316 (3)	0.579 (2)	C(12)	0.275 (3)	0.043 (3)	−0.009 (2)
C(3)	0.681 (5)	0.290 (2)	0.622 (2)	C(13)	0.187 (3)	0.120 (2)	−0.041 (1)

Table II (Continued)

atom	x	y	z	atom	x	y	z
			Molecule 2b				
C(14)	0.097 (2)	0.145 (2)	−0.007 (1)	C(41)	0.160 (1)	0.360 (1)	0.684 (1)
C(15)	0.122 (2)	0.093 (2)	0.049 (2)	C(42)	0.186 (2)	0.450 (2)	0.671 (1)
C(16)	0.277 (3)	0.370 (2)	0.036 (1)	C(43)	0.153 (2)	0.464 (2)	0.593 (2)
C(17)	0.191 (2)	0.407 (2)	0.076 (2)	C(44)	0.094 (2)	0.376 (2)	0.521 (1)
C(18)	0.254 (3)	0.446 (2)	0.162 (2)	C(45)	0.072 (2)	0.277 (2)	0.528 (1)
C(19)	0.383 (3)	0.434 (2)	0.177 (2)	C(46)	0.104 (2)	0.273 (2)	0.607 (1)
C(20)	0.398 (3)	0.385 (2)	0.096 (2)	C(51)	0.090 (1)	0.282 (1)	0.780 (1)
C(21)	0.772 (2)	0.152 (2)	0.295 (1)	C(52)	0.076 (2)	0.165 (2)	0.741 (1)
C(22)	0.778 (2)	0.201 (2)	0.235 (1)	C(53)	−0.016 (2)	0.104 (2)	0.742 (1)
C(23)	0.653 (2)	0.248 (2)	0.191 (1)	C(54)	−0.096 (2)	0.161 (2)	0.786 (1)
C(24)	0.168 (2)	0.167 (2)	0.248 (1)	C(55)	−0.087 (2)	0.274 (2)	0.826 (1)
C(25)	0.167 (2)	0.195 (2)	0.334 (1)	C(56)	0.006 (2)	0.335 (1)	0.826 (1)
C(26)	0.297 (2)	0.229 (2)	0.407 (1)	C(61)	0.214 (2)	0.479 (1)	0.847 (1)
C(31)	0.337 (1)	0.281 (1)	0.792 (1)	C(62)	0.118 (2)	0.558 (1)	0.834 (1)
C(32)	0.368 (2)	0.205 (1)	0.832 (1)	C(63)	0.123 (2)	0.669 (2)	0.896 (1)
C(33)	0.482 (2)	0.143 (2)	0.841 (1)	C(64)	0.226 (2)	0.697 (2)	0.969 (1)
C(34)	0.569 (2)	0.160 (2)	0.811 (1)	C(65)	0.325 (2)	0.622 (2)	0.985 (1)
C(35)	0.545 (2)	0.236 (2)	0.776 (1)	C(66)	0.315 (2)	0.514 (1)	0.920 (1)
C(36)	0.432 (2)	0.295 (1)	0.764 (1)	R(1)	0.200 (2)	0.350 (2)	0.775 (1)

By analogy to the results previously described for the analogous reactions with diols,[18] dimeric zirconocene dithiolate complexes are suggested for the present products **1**. In the case of the reactions of $HS(CH_2)_nSH$ (n = 2, 3), the formulations of the resulting zirconocene dithiolates, **1a** and **1b**, respectively, have been confirmed to be dimeric by X-ray crystallographic studies (vide infra). The dimeric compounds **1a** and **1b** can also be prepared from the reactions of Cp_2ZrMe_2 with the disymmetric reagents $HS(CH_2)_nSSiMe_3$ (n = 2, 3). These reaction proceed with the elimination of methane and TMS. Alternatively, reaction of the commercially available reagent $[Cp_2ZrHC]_n$ with $HS(CH_2)_nSSiMe_3$ (n = 2, 3) proceeds with elimination of H_2 and Me_3SiCl, affording the compounds **1a** and **1b**.

The mechanism of formation of the Zr–dithiolate species is not understood; however, the reactions where a Zr–S bond is formed via an elimination of CH_4, Me_4Si, H_2, or Me_3SiCl are thought to proceed through a four-center intermediate (C). The apparent preference for dimeri-

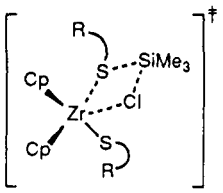

C

zation as opposed to chelate ring closure (i.e. monomer formation) may arise from a steric bias for an exo orientation of the substituents on sulfur, although kinetic factors cannot be excluded at this point. The nature of the intermediate species in the formation of the dimers is not known. But, the reactions of Cp_2ZrMe_2 with 1 equiv of thiol have been shown to proceed with evolution of methane, affording the complex $Cp_2ZrMe(SR)$.[28] In the present reactions involving dithiols an intermediate $Cp_2ZrMe(\mu\text{-}SRS)MeZrCp_2$ is postulated but has not been observed or isolated. In the related reactions of diols with Cp_2TiPh_2 an analogue of the proposed intermediate, that is, $Cp_2TiPh(\mu\text{-}OCH_2C(CH_3)_2CH_2O)PhTiCp_2$, has been isolated and crystallographically studied.[29]

Structural Studies of 1a and 1b. An ORTEP drawing of the dimeric molecule **1a** is shown in Figure 1. The Zr

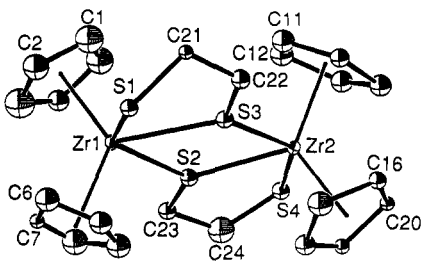

Figure 1. ORTEP drawing of **1a**. 30% thermal ellipsoids are shown; hydrogen atoms are omitted for clarity.

atom separation within the dimeric molecule is found to be 4.536 Å. Two π-bonded cyclopentadienyl rings and three sulfur atoms complete the coordination sphere of the Zr centers. One sulfur atom forms a terminal Zr–S bond, while the other two bridge the two metal centers. The Zr–C bond distances are typical. The terminal Zr–S separations are found to be 2.56 (1) and 2.676 (1) Å. The Zr–S distances found for **1a** are similar to those found in $(Cp_2Zr(SPh))_2(\mu\text{-}O)$[30] (2.542 (2) and 2.554 (2) Å) and $Cp_2Zr(SCHMe)PMe_3$[28] (2.529 (3) Å). These terminal Zr–S bond distances in **1a** are in the range found for the average bridging Zr–S distances, 2.68 (1) Å. Although one might intuitively expect to observe discernible differences in the two types of Zr–S bonds, the disorder in the bridging sulfur locations in the present study masks these structural details. Discussion of the degree of planarity of the $Zr(\mu\text{-}S_2)Zr$ core is also precluded by the disorder in the solid-state structure of **1a**. The bite angles at Zr formed by the chelation of the ethanedithiolate ligands were determined to range from 69.3 (4) to 76.1 (4)°. These S–Zr–S angles are slighty smaller than those observed in simpler complexes containing five-membered chelate rings. The S(2)–Zr–S(3) angles ranged from 60.9 (4) to 67.1 (4)°, which are also significantly smaller than the S–Zr–S angle of 89.5 (2)° found in the Zr_2S_2 core of $(Cp_2Zr(\mu\text{-}S))_2$.[31] The smaller S–Zr–S angle is attributed to the dimeric nature of **1a**, which presents steric crowding about Zr and thus impinges on the angles. The determination of the angles between the ZrS_3 planes in **1a** is precluded by the disorder in the bridging atom sites. However, as a general comment, the maximum angle between these planes involving the various sites was found to be 27°.

(28) Buchwald, S. L.; Neilsen, R. B.; Dewan, J. C. *J. Am. Chem. Soc.* **1987**, *109*, 1590.
(29) Nadasdi, T. T.; Stephan, D. W. *Can. J. Chem.* **1991**, *69*, 167.
(30) Petersen, J. L. *J. Organomet. Chem.* **1979**, *166*, 179.
(31) Bottomley, F.; Drummond, D. F.; Egharevba, G. O.; White, P. S. *Organometallics* **1986**, *5*, 1620.

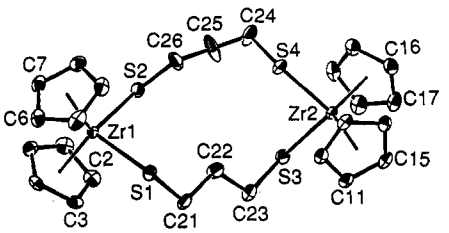

Figure 2. ORTEP drawing of **1b**. 30% thermal ellipsoids are shown; hydrogen atoms are omitted for clarity.

The lack of precise, structural data for the bridging sulfur atoms affords two possible descriptions of **1a**; associated monomers (AM) or a twisted dimer (TD). The

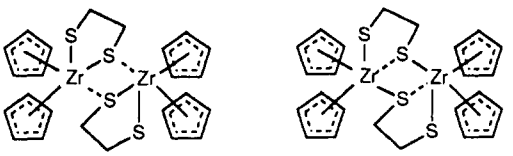

AM TD

former description is consistent with the small bite angle for ethanedithiolate and the known Lewis acidity of Zr. However, if **1a** is truly constituted from associated monomers, one might anticipate a monomer/dimer equilibrium for which there is no evidence. The alternate description, that is, the twisted dimer or macrocycle, is consistent with the extremely poor solubility of **1a**. This issue is addressed further by examination of the complexation chemistry (vide infra).

An ORTEP drawing of **1b** is shown in Figure 2. The molecule contains two typical Cp_2Zr units. Two sulfur atoms complete the coordination sphere of Zr. It is the linkage of the two metal centers by the propanedithiolate chains that form a 12-membered macrocycle. The Zr···Zr distance is 7.570 (1) Å.

The Zr–S distances in **1b** are slightly shorter than those observed for **1a**. This is attributable to the greater Lewis acidity of the Zr centers in **1b** arising from the absence of bridging donor atoms. The Zr–S bond lengths in **1a** and **1b** are significantly longer than the Zr–S distances of 2.490 (3) and 2.482 (3) Å found in $(Cp_2Zr(\mu\text{-}S))_2$, consistent with simple charge/donor arguments. In contrast, the Zr–S distances found in $Cp_2ZrCl(S_2CP(SiMe_3)_2)$[32] (2.733 (7) and 2.640 (8) Å) are significantly longer than those found in either **1a** or **1b**, consistent with the poorer donor ability of the phosphinodithioformato ligand compared to thiolate.

The alkyl substituents on the sulfur atoms in **1b** adopt an *endo-transoid* conformation. A similar disposition was observed for $Cp_2Zr(\mu\text{-}OCH_2C(CH_3)_2CH_2O)_2ZrCp_2$.[18] In that case the geometry was attributed to the domination of the electronic preference for an *endo* conformation (D)

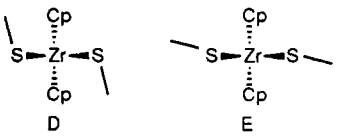

D E

arising from Zr–O π-bonding effects over the steric restrictions which favor an *exo* disposition (E). A postulate of similar Zr–S π bonding is not supported by the structural data. The Zr–S distances in **1b** average 2.504 (2) Å, while a Zr–O distance of 1.945 (6) Å is found in $Cp_2Zr(\mu\text{-}OCH_2C(CH_3)_2CH_2O)_2ZrCp_2$.[18] The Zr–S–C angles in **1b** average 112.4° in contrast to the Zr–O–C angle in $Cp_2Zr(\mu\text{-}OCH_2C(CH_3)_2CH_2O)_2ZrCp_2$,[18] which was found to be 142.5 (1)°. Compared to the related alkoxide macrocycle, the steric interactions between the alkyl chains and the cyclopentadienyl rings in **1b** are diminished as a result of the greater Zr–S bond length. Such considerations may offer reasons as to why the *exo* conformation is tolerated in **1b**. Nonetheless, the driving force behind the adoption of this geometry are not clearly understood.

Scheme I

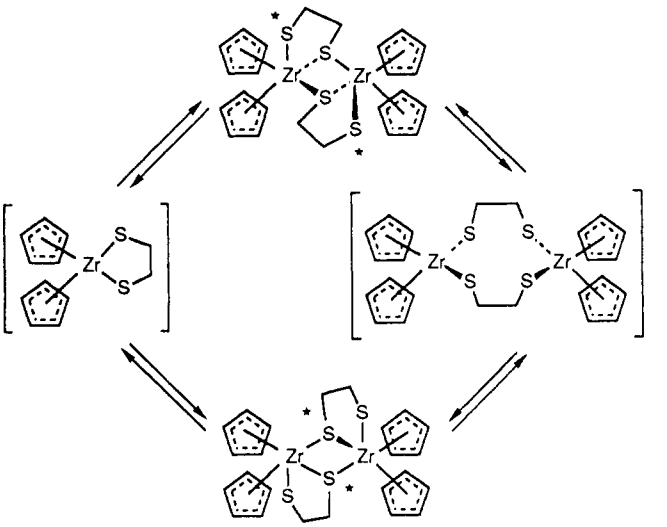

In contrast to the situation seen in **1a**, the angle between the ZrS_2 planes of the two Zr coordination spheres in **1b** was found to be 92.9°. Further, relative to the macrocyclic ring the four sulfur atoms adopt *endodentate* positions. These structural features suggest that the early-metal macrocycle **1b** is preorganized for encapsulation of a late metal in a pseudotetrahedral environment. This feature was investigated via complexation of silver (vide infra).

The compounds **1a** and **1b** show two structural types for a dimeric formulation. Erker and Noe[33] have shown that related binuclear endiolato– and catecholato–zirconocene complexes exhibit a structure analogous to that of **1a** in solution and that such compounds are fluxional. Variable-temperature NMR studies of **1b** showed no variation with temperature in the range 233–333 K. However, on warming of samples to 333 K, the ^1H NMR resonances attributable to the methylene protons of **1a** broadened and began to shift toward each other. Temperature range and solubility limitations precluded the observation of coalescence, and thus, activation parameters were not obtained. Nonetheless, these data suggest a dynamic process in which the methylene resonances are averaged. The intermediate in such a process may be the open macrocycle similar in structure to that of **1b**. Alternatively, mononuclear intermediates are possible. The two possibilities are shown in Scheme I. Erker and Noe[33] observed dramatically different activation energies for the two processes in their systems. Although the lack of activation barrier data for **1a** precludes a conclusive assessment, the complexation chemistry of **1a** and the structure of **1b** favor the postulate of a macrocyclic intermediate.

Complexation of 1a and 1b. Despite the fact that either **1a** nor **1b** is discernibly soluble in methylene chloride or THF, addition of $AgBPh_4$ in THF to a methylene chloride suspension of **1a** or **1b** results in reaction. Gradually ovr a 3–4-h period the solution becomes in-

(32) Hey, E.; Lappert, F.; Atwood, J. L.; Bott, S. G. *J. Chem. Soc., Chem. Commun.* **1987**, 421.

(33) Communication prior to publication: Erker, G.; Noe, R. *J. Chem. Soc. D*, in press.

Table III. Selected Bond Distances and Angles for Molecules 1a–2b

			Bond Distances for 1a				
Zr(1)–S(1)	2.56 (1)	Zr(2)–C(17)	2.59 (2)	Zr(1)–C(7)	2.47 (2)	S(4)–C(24)	1.89 (2)
Zr(1)–S(2A)	2.76 (2)	Zr(2)–C(18)	2.55 (2)	Zr(1)–C(8)	2.49 (2)	C(21)–C(22)	1.46 (6)
Zr(1)–S(2B)	2.69 (2)	Zr(2)–C(19)	2.48 (2)	Zr(1)–C(9)	2.55 (2)	C(23)–C(24)	1.52 (3)
Zr(1)–S(3A)	2.58 (1)	Zr(2)–C(20)	2.48 (2)	Zr(1)–C(10)	2.56 (2)	Zr(2)–S(2A)	2.67 (2)
Zr(1)–S(3B)	2.61 (1)	S(1)–C(21)	1.65 (4)	Zr(2)–S(2B)	2.72 (2)	Zr(2)–S(3A)	2.63 (1)
Zr(1)–C(1)	2.58 (2)	Zr(1)–C(2)	2.56 (2)	Zr(2)–S(3B)	2.80 (2)	Zr(2)–S(4)	2.676 (8)
S(2A)–C(23)	1.71 (3)	Zr(1)–C(3)	2.49 (2)	Zr(2)–C(11)	2.63 (2)	Zr(2)–C(12)	2.54 (2)
S(2B)–C(23)	1.87 (3)	Zr(1)–C(4)	2.48 (2)	Zr(2)–C(13)	2.52 (2)	Zr(2)–C(14)	2.59 (2)
Zr(1)–C(5)	2.53 (2)	S(3A)–C(22)	1.98 (3)	Zr(2)–C(15)	2.65 (2)		
Zr(1)–C(6)	2.51 (2)	S(3B)–C(22)	1.86 (4)				
			Bond Angles for 1a				
S(1)–Zr(1)–S(2A)	135.8 (4)	S(1)–Zr(1)–S(2B)	130.5 (4)	Zr(1)–S(2B)–Zr(2)	113.9 (5)	Zr(2)–S(2B)–C(23)	107 (1)
S(2B)–Zr(1)–S(3A)	62.8 (4)	S(1)–Zr(1)–S(3A)	75.1 (4)	Zr(1)–S(2B)–C(23)	121.3 (9)	Zr(1)–S(3A)–Zr(2)	121.0 (4)
S(2B)–Zr(1)–S(3B)	62.5 (5)	S(1)–Zr(1)–S(3B)	69.5 (5)	Zr(1)–S(3A)–C(22)	112 (1)	Zr(2)–S(3A)–C(22)	122 (1)
S(2A)–Zr(1)–S(3A)	60.9 (4)	S(2A)–Zr(1)–S(3B)	67.1 (5)	Zr(1)–S(3B)–Zr(2)	113.9 (5)	Zr(1)–S(3B)–S(3A)	115 (1)
S(2A)–Zr(2)–S(3A)	61.4 (4)	S(2A)–Zr(2)–S(3B)	65.7 (4)	Zr(1)–S(3B)–C(22)	115 (1)	Zr(2)–S(3B)–C(22)	120 (1)
S(3A)–Zr(2)–S(4)	129.5 (3)	S(2A)–Zr(2)–S(4)	69.3 (4)	Zr(2)–S(4)–C(24)	103.7 (7)	S(1)–C(21)–C(22)	124 (3)
S(3B)–Zr(2)–S(4)	134.5 (4)	S(2B)–Zr(2)–S(3A)	61.6 (4)	S(3A)–C(22)–C(21)	101 (2)	S(3B)–C(22)–C(21)	104 (3)
S(2B)–Zr(2)–S(3B)	59.7 (4)	S(2B)–Zr(2)–S(4)	76.1 (4)	S(2A)–C(23)–C(24)	115 (2)	S(2B)–C(23)–C(24)	106 (1)
Zr(1)–S(1)–C(21)	109 (1)	Zr(2)–S(2A)–Zr(1)	113.1 (5)	S(4)–C(24)–C(23)	108 (2)		
Zr(1)–S(2A)–C(23)	125 (1)	Zr(1)–S(2A)–Zr(2)	113.1 (5)				
			Bond Distances for 1b				
Zr(1)–S(1)	2.515 (2)	S(3)–C(23)	1.802 (8)	Zr(2)–C(13)	2.514 (6)	Zr(2)–C(14)	2.497 (6)
Zr(1)–S(2)	2.482 (2)	S(4)–C(24)	1.817 (7)	Zr(2)–C(15)	2.496 (6)	Zr(2)–C(16)	2.499 (6)
Zr(1)–C(1)	2.508 (6)	Zr(1)–C(2)	2.504 (6)	Zr(2)–C(17)	2.509 (6)	Zr(2)–C(18)	2.496 (6)
Zr(1)–C(3)	2.507 (6)	Zr(1)–C(4)	2.483 (6)	Zr(2)–C(19)	2.507 (6)	C(21)–C(22)	1.563 (9)
Zr(1)–C(5)	2.501 (6)	Zr(1)–C(6)	2.511 (6)	Zr(2)–C(20)	2.514 (6)	C(22)–C(23)	1.490 (9)
Zr(1)–C(7)	2.489 (6)	Zr(1)–C(8)	2.520 (6)	S(1)–C(21)	1.811 (7)	C(24)–C(25A)	1.37 (1)
Zr(1)–C(9)	2.514 (6)	Zr(1)–C(10)	2.510 (6)	S(2)–C(26)	1.819 (8)	C(24)–C(25B)	1.42 (2)
Zr(2)–S(3)	2.518 (2)	Zr(2)–S(4)	2.499 (2)	C(25A)–C(26)	1.64 (1)	C(25B)–C(26)	1.43 (2)
Zr(2)–C(11)	2.516 (5)	Zr(2)–C(12)	2.520 (6)				
			Bond Angles for 1b				
S(1)–Zr(1)–S(2)	99.87 (5)	S(3)–Zr(2)–S(4)	100.86 (6)	S(3)–C(23)–C(22)	112.6 (5)	S(4)–C(24)–C(25A)	117.2 (6)
Zr(1)–S(1)–C(21)	113.0 (2)	Zr(1)–S(2)–C(26)	109.6 (3)	S(4)–C(24)–C(25B)	119.4 (9)	C(24)–C(25A)–C(26)	111.6 (7)
Zr(2)–S(3)–C(23)	114.9 (3)	Zr(2)–S(4)–C(24)	112.2 (3)	C(24)–C(25B)–C(26)	122 (1)	S(2)–C(26)–C(25A)	102.2 (6)
S(1)–C(21)–C(22)	110.4 (5)	C(21)–C(22)–C(23)	113.1 (6)	S(2)–C(26)–C(25B)	135.2 (9)		
			Bond Distances for 2a				
Ag(1)–Zr(1)	3.047 (2)	Zr(2)–C(17)	2.49 (2)	Zr(1)–C(3)	2.49 (2)	Zr(1)–C(4)	2.46 (2)
Ag(1)–Zr(2)	3.058 (2)	Zr(2)–C(18)	2.49 (2)	Zr(1)–C(5)	2.46 (2)	Zr(1)–C(6)	2.50 (2)
Ag(1)–S(1)	2.514 (5)	Zr(2)–C(19)	2.49 (2)	Zr(1)–C(7)	2.51 (2)	Zr(1)–C(8)	2.47 (2)
Ag(1)–S(2)	2.489 (5)	Zr(2)–C(20)	2.52 (2)	Zr(1)–C(9)	2.50 (2)	Zr(1)–C(10)	2.52 (2)
Ag(1)–S(3)	2.479 (5)	S(1)–C(21)	1.85 (2)	Zr(2)–S(3)	2.560 (5)	Zr(2)–S(4)	2.617 (5)
Ag(1)–S(4)	2.497 (5)	S(2)–C(23)	1.84 (2)	Zr(2)–C(11)	2.51 (2)	Zr(2)–C(12)	2.51 (2)
Zr(1)–S(1)	2.588 (5)	S(3)–C(24)	1.81 (2)	Zr(2)–C(13)	2.46 (2)	Zr(2)–C(14)	2.47 (2)
Zr(1)–S(2)	2.597 (5)	S(4)–C(22)	1.84 (2)	Zr(2)–C(15)	2.50 (2)	Zr(2)–C(16)	2.48 (2)
Zr(1)–C(1)	2.52 (2)	Zr(1)–C(2)	2.51 (2)	C(21)–C(22)	1.59 (3)	C(23)–C(24)	1.51 (2)
			Bond Angles for 2a				
Zr(1)–Ag(1)–Zr(2)	170.96 (8)	Zr(1)–Ag(1)–S(3)	120.4 (1)	Ag(1)–S(2)–C(23)	93.4 (6)	Ag(1)–S(2)–Zr(1)	73.6 (1)
Zr(1)–Ag(1)–S(4)	130.2 (1)	Zr(2)–Ag(1)–S(1)	121.3 (1)	Zr(1)–S(2)–C(23)	118.9 (7)	Ag(1)–S(3)–Zr(2)	74.7 (1)
Zr(2)–Ag(1)–S(2)	128.8 (1)	S(1)–Ag(1)–S(2)	109.3 (2)	Ag(1)–S(3)–C(24)	92.7 (6)	Zr(2)–S(3)–C(24)	119.0 (7)
S(1)–Ag(1)–S(3)	124.8 (2)	S(1)–Ag(1)–S(4)	92.6 (2)	Ag(1)–S(4)–Zr(2)	73.4 (1)	Zr(2)–S(4)–C(22)	118.0 (6)
S(2)–Ag(1)–S(3)	91.8 (2)	S(2)–Ag(1)–S(4)	133.5 (2)	Ag(1)–S(4)–C(22)	93.5 (6)	S(1)–C(21)–C(22)	111 (1)
S(3)–Ag(1)–S(4)	108.9 (2)	S(1)–Zr(1)–S(2)	103.8 (2)	S(4)–C(22)–C(21)	112 (1)	S(2)–C(23)–C(24)	114 (1)
S(3)–Zr(2)–S(4)	102.9 (2)	Ag(1)–S(1)–Zr(1)	73.3 (1)	S(3)–C(24)–C(23)	112 (1)		
Ag(1)–S(1)–C(21)	91.1 (6)	Zr(1)–S(1)–C(21)	118.1 (6)				
			Bond Distances for 2b				
Ag(1)–Zr(1)	3.333 (3)	Zr(2)–C(17)	2.48 (2)	Zr(1)–C(5)	2.52 (2)	Zr(1)–C(6)	2.53 (2)
Ag(1)–Zr(2)	3.280 (3)	Zr(2)–C(18)	2.52 (2)	Zr(1)–C(7)	2.52 (2)	Zr(1)–C(8)	2.50 (2)
Ag(1)–S(1)	2.590 (5)	Zr(2)–C(19)	2.53 (2)	Zr(1)–C(9)	2.48 (2)	Zr(1)–C(10)	2.46 (2)
Ag(1)–S(2)	2.657 (5)	Zr(2)–C(20)	2.49 (2)	Zr(2)–S(3)	2.551 (5)	Zr(2)–S(4)	2.559 (5)
Ag(1)–S(3)	2.658 (5)	S(1)–C(21)	1.89 (2)	Zr(2)–C(11)	2.48 (2)	Zr(2)–C(12)	2.55 (2)
Ag(1)–S(4)	2.599 (5)	S(2)–C(26)	1.83 (2)	Zr(2)–C(13)	2.47 (2)	Zr(2)–C(14)	2.48 (2)
Zr(1)–S(1)	2.550 (5)	S(3)–C(23)	1.82 (2)	Zr(2)–C(15)	2.49 (2)	Zr(2)–C(16)	2.48 (2)
Zr(1)–S(2)	2.550 (5)	S(4)–C(24)	1.83 (2)	C(21)–C(22)	1.48 (3)	C(22)–C(23)	1.50 (3)
Zr(1)–C(1)	2.52 (2)	Zr(1)–C(2)	2.49 (2)	C(24)–C(25)	1.47 (3)	C(25)–C(26)	1.56 (3)
Zr(1)–C(3)	2.49 (2)	Zr(1)–C(4)	2.47 (2)				
			Bond Angles for 2b				
Zr(1)–Ag(1)–Zr(2)	178.05 (8)	S(1)–Zr(1)–S(2)	101.7 (2)	Zr(1)–S(2)–C(26)	114.6 (7)	Ag(1)–S(3)–Zr(2)	78.0 (1)
S(1)–Ag(1)–S(2)	97.8 (2)	S(1)–Ag(1)–S(3)	92.3 (2)	Ag(1)–S(3)–C(23)	94.1 (7)	Zr(2)–S(3)–C(23)	118.8 (7)
S(1)–Ag(1)–S(4)	145.9 (2)	S(2)–Ag(1)–S(3)	144.3 (2)	Ag(1)–S(4)–C(24)	94.0 (6)	Ag(1)–S(4)–Zr(2)	79.0 (1)
S(2)–Ag(1)–S(4)	91.1 (2)	S(3)–Ag(1)–S(4)	99.5 (2)	Zr(2)–S(4)–C(24)	116.6 (6)	S(1)–C(21)–C(22)	111 (1)
S(3)–Zr(2)–S(4)	103.4 (2)	Ag(1)–S(1)–Zr(1)	80.9 (1)	C(21)–C(22)–C(23)	115 (2)	S(3)–C(23)–C(22)	115.1 (1)
Ag(1)–S(1)–C(21)	94.3 (5)	Zr(1)–S(1)–C(21)	116.7 (7)	S(4)–C(24)–C(25)	111 (1)	C(24)–C(25)–C(26)	117 (2)
Ag(1)–S(2)–Zr(1)	79.6 (5)	Ag(1)–S(2)–C(26)	94.6 (6)	S(2)–C(26)–C(25)	109 (1)		

creasingly yellow in color and the amount of zirconocene dithiolate on the bottom of the vessel diminishes. Following filtration, addition of THF/hexane affords beautiful, pale yellow blocks of **2a** and **2b**, respectively. The

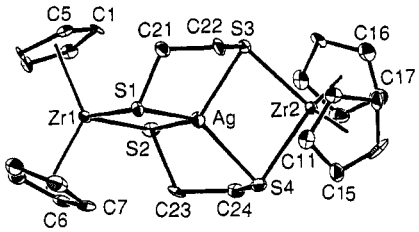

Figure 3. ORTEP drawing of the cation of **2a**. 30% thermal ellipsoids are shown; hydrogen atoms are omitted for clarity.

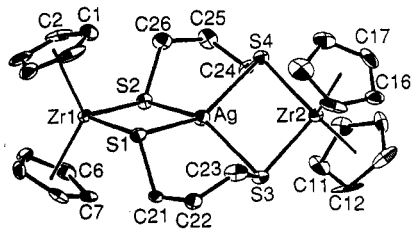

Figure 4. ORTEP drawing of the cation of **2b**. 30% thermal ellipsoids are shown; hydrogen atoms are omitted for clarity.

^{1}H NMR spectra of **2a** and **2b** are consistent with the formulation of these products as $AgBPh_4$ salts of **1a** and **1b**, respectively. While the spectral data imply some

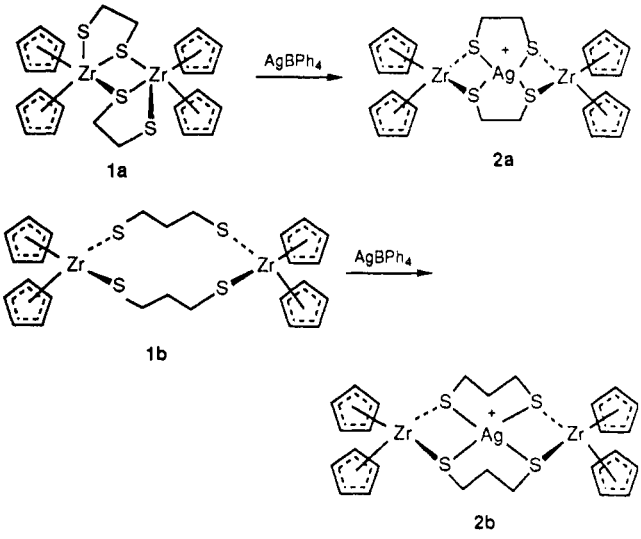

molecular symmetry, the nature of the interaction between silver and the zirconocene dithiolate was unclear. Confirmation of the formulations and the elucidation of the precise nature of these products was achieved via crystallographic study (vide infra). Attempts to form other metal salts of **1a** and **1b** led only to the formation of insoluble products. For example, reactions with either $AgBF_4$ or $AgPF_6$ gives insoluble, pale yellow powders, while reaction with $[Pd(NCMe)_4][BF_4]_2$ gives a totally insoluble, brick red precipitate. In each case, these products were not characterized but presumed to be the analogous metal BF_4 or PF_6 salts. While the problem of solubility of these macrocyclic metalloligands and their complexes is overcome by the use of the BPh_4 anion, efforts are underway to prepare analogous macrocycles that incorporate substituted cyclopentadienyl moieties.

Structural Studies of 2a and 2b. ORTEP drawings of the cations of **2a** and **2b** are shown in Figures 3 and 4, respectively. In both complexes, the bond distances and angles within the anion, as well as the cyclopentadienyl groups of the cation, are typical and require no further comment. The cations of **2a** and **2b** are similar. The central Ag ion is coordinated to four sulfur atoms each of

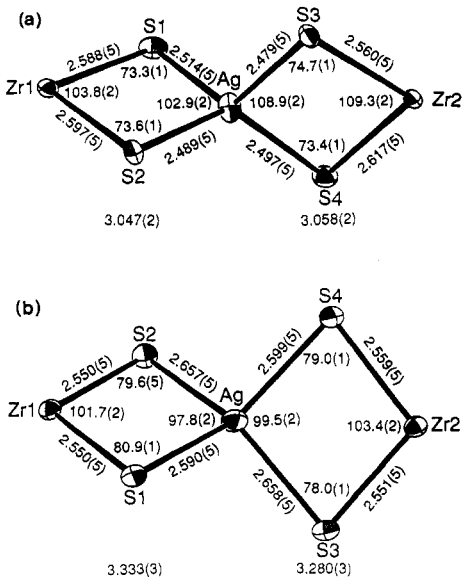

Figure 5. Structural details of the cores of the cation of (a) **2a** and (b) **2b**. Distances are given in angstroms, and angles, in degrees.

which bridges to a Zr center. Each of the two Zr centers are bonded to two sulfurs in addition to the two π-bonded cyclopentadienyl ligands. Thus, in either case, the zirconocene dithiolate acts as a macrocyclic metalloligand to encapsulate the silver ion.

While the gross features of **2a** and **2b** are similar, the details of the metal coordination spheres are not. Some of the structural details of the $Zr(\mu\text{-}S)_2Ag(\mu\text{-}S)_2Zr$ cores of **2a** and **2b** are illustrated in Figure 5. In the case of **2a**, the Zr–Ag–Zr chain is not linear, forming an angle at Ag of 170.96 (8)°. In contrast, in **2b** the Zr–Ag–Zr angle is 178.05 (8)°. The greater ring strain caused by the adjacent 4,5,4,5-membered rings in **2a** is accommodated by this distortion from linearity, while, in **2b**, a linear arrangement is tolerated by the 4,6,4,6-ring system.

The angle between the pair of ZrS_2 planes in **2a** and **2b** is 115.5 and 133.0°, respectively. In the case of **2a**, this requires a dramatic reorientation of the ligand upon complexation of silver. In contrast, the geometry of **2b** is only slightly perturbed by complexation. Reorientation of the methylene chains and a closer approach of the two Zr centers require a small twist of the ZrS_2 planes relative to each other to avoid steric conflicts.

The Zr–S and Ag–S distances average 2.590 (10) and 2.495 (10) Å in **2a** and 2.552 (10) and 2.628 (10) Å, respectively, in **2b**. These Zr–S distances are slightly longer than those found in **1b** as expected for bridging, thiolate moieties. Not unexpectedly, the Ag–S distances in **2a** and **2b** are shorter than those found in the homoleptic pseudooctahedral complexes $[Ag([9]aneS_3)_2]^+$ [34] (2.697 (5) and 2.753 (4) Å) and $[Ag([18]aneS_6)]^+$ [35] (2.6665 (12) and 2.7813 (10) Å). The only previously known compound that contains a pseudotetrahedral AgS_4 coordination sphere is the complex $[Ag_3([9]aneS_3)_3]^{3+}$ described by Wieghardt et al.[36] The range of observed for the Ag–S distances in that species (2.724 (2), 2.595 (4), 2.613 (4), and 2.480 (2) Å) is similar to that seen in **2a** and **2b**. In unpublished work, Loeb et al.[37] have recently characterized the related hom-

(34) Clarkson, J. A.; Yagbasan, R.; Blower, P. J.; Rawle, S. C.; Cooper, S. R. *J. Chem. Soc., Chem. Commun.* **1987**, 950.
(35) Blake, A. J.; Gould, R. O.; Holder, A. J.; Hyde, T. I.; Schröder, M. *Polyhedron* **1989**, *8*, 513.
(36) Küppers, H.-J.; Wieghardt, K.; Tsay, Y.-H.; Krüger, C.; Nuber, B.; Weiss, J. *Angew. Chem., Int. Ed. Engl.* **1987**, *26*, 575.

oleptic complex $[Ag([16]aneS_4)]^+$, where the average Ag–S distance was found to be 2.550 (1) Å.

The angles about Ag in both **2a** and **2b** fall into three categories. In the case of **2a** there are two angles at about 92°, two at about 109°, and two at about 130°. In **2b**, the three pairs range around 92, 99, and 145°. In both cases, the geometry about Ag is best described as pseudotetrahedral with a distortion toward square planar. Similar, but less dramatic, "flattening" of the Ag coordination sphere is also observed for $[Ag([16]aneS_4)]^+$.[37] This flattening of the Ag coordination sphere for **2b** suggests that the metalloligand **1b** might also bind group 8 metals where a square-planar coordination sphere is demanded. In the case of **1a**, the ring strain is likely to preclude such complexation. This postulate is consistent with the observations made for the related metalloligands $Cp_2Ti(SCH_2CH_2PPh_2)_2$ and $Cp_2Ti(SCH_2CH_2CH_2PPh_2)_2$.[14-16]

The S–Zr–S angles were found to be 103.8 (2) and 109.3 (2)° in **2a** and 103.4 (2) and 101.7 (2)° in **2b**. These values are much larger than the corresponding angles found in $(Cp_2Ti(\mu\text{-}SMe)_2)_2Ni$[12] (98.6 (1)°) and $[(Cp_2Nb(\mu\text{-}SMe_2)_2Ni]^{2+}$[38] (98.0 (3)°) and comparable to those found in $[(Cp_2Ta(\mu\text{-}SMe_2)_2Pt]^{2+}$[39] (104 (1) and 105 (1)°). The Zr–S–Ag angles in **2a** average 73.8 (2)°. These are comparable to the corresponding angles in $(Cp_2Ti(\mu\text{-}SMe)_2)_2Ni$,[12] which were found to be 72.0 (1)°, while in $[(Cp_2Nb(\mu\text{-}SMe)_2)_2Ni]^{2+}$[38] the Nb–S–Ni angles average 72.5 (6)°. In contrast, the Zr–S–Ag angles in **2b** average 79.4 (2)°. Similar angles at S were seen in $[Cp_2Ti(\mu\text{-}SCH_2CH_2PPh_2)_2Cu]^+$[14] (78.1 (1) and 78.0 (1)°) and $[Cp_2Ti(\mu\text{-}SCH_2CH_2CH_2PPh_2)_2Rh]^+$[16] (81.6 (1) and 81.5 (1)°). Distortion of the angles about the cores of d^0–d^{10} heterobimetallics and, in particular, angles at the bridging atoms of less than 80° have been discussed previously as indicators of dative bonding interactions between the metal centers. On the basis of these criteria, the above data suggest that such dative interactions may be present in **2a** and **2b**. Clearly, a second important indicator of such dative interactions is the metal–metal separations. In **2a**, the Zr–Ag distances were found to be 3.047 (2) and 3.058 (2) Å, while in **2b** the metal–metal separations are 3.333 (3) and 3.280 (3) Å. For comparative purposes, in the related d^0–d^{10} thiolate-bridged heterobimetallics $[Cp_2Ti(\mu\text{-}SCH_2CH_2CH_2PPh_2)_2Ni]$,[15] $(Cp_2Ti(\mu\text{-}SMe)_2)_2Ni$,[12] $[Cp_2Ti(\mu\text{-}SMe)_2Cu(NCMe)_2]^+$,[13] $[Cp_2Ti(\mu\text{-}SCH_2CH_2PPh_2)_2Cu]^+$,[14] $[Cp_2Ti(\mu\text{-}SMe)_2CuPPh_3]^+$,[11] and $[Cp_2Ti(\mu\text{-}SMe)_2CuPCy_3]^+$[11] the metal–metal separations were found to be 2.825 (2), 2.786 (1), 2.846 (2), 3.024 (1), 2.803 (1), and 2.840 (1) Å, respectively. A significantly greater degree of dative donation from Ag to Zr appears to account for the greater distortions of the Zr–S–Ag angles and the closer proximity of the Zr and Ag in **2a**. The postulate of metal–metal interactions in such trimetallic species is supported by the recent report of EHMO calculations for the species $(Cp_2Zr(\mu\text{-}PH_2)_2)_2Ni$[40] and by preliminary results of similar calculations for a related variety of d^0–d^{10}, thiolate-bridged heterobimetallics.[41] In the present compounds, the role of the macrocycle in altering the metal–metal interaction is of interest. Presumably, the tight geometric constraints imposed by the macrocyclic ring **1a** enhance such dative interactions; however, further discussion of this aspect hinges on the nature of the related compounds $[(Cp_2Zr((\mu\text{-}SR)_2)_2Ag]^+$, where the macrocyclic effect is absent. Such analogues have not, as yet, been synthesized.

The coordination environment offered by the present ligands suggests the analogy to crown thioethers. It has been recently demonstrated by Gellman et al.[42] that simple methyl substituents on the periphery of crown thioethers encourage sulfur atoms to adopt *endodentate* positions in the free ligands and that such structural features enhance the ability of the macrocycles to bind metals. In the present ligands, the Cp_2Zr moieties act in a similar manner precipitating the endodentate nature of the sulfur atoms. Of course, for **1a**, the Lewis acidity of the Zr center also affects the geometry of the free ligand. In the derived silver complex **2a**, the S···S distances within the five-membered chelate rings (S1···S3 = 4.424 (7) Å; S2···S4 = 4.582 (7) Å) compare with those within the four-membered ZrS_2Ag rings (S1···S2 = 4.080 (7) Å; S3···S4 = 4.050 (7) Å). The S···S distances within the six-membered rings in **2b** (S1···S3 = 3.784 (7) Å; S2···S4 = 3.752 (7) Å) are similar to those between sulfur atoms on each Zr center (S1···S2 = 3.954 (7) Å; S3···S4 = 4.012 (7) Å). This suggests the $Cp_2Zr(SR)_2$ moiety is similar in bite to a three-carbon chain. This leads to the likening of **1a** and **1b** to metalated versions of $[14]aneS_4$ and $[16]andS_4$, respectively.

Summary. The present results offer synthetic routes to a new class of macrocyclic ligands. Further, the data confirms that these early-metal macrocycles act as effective metalloligands for the encapsulation of other metals. The participation of the early metal in reactions centered on the late metal are the subject of present study.

Acknowledgment. Financial support from the NSERC of Canada is gratefully acknowledged. The University of Windsor in thanked for the award of a Research Professorship.

Supplementary Material Available: Tables of thermal and hydrogen atom parameters and bond distances and angles associated with the BPh_4 anions (14 pages); listings of values of $10F_o$ and $10F_c$ (72 pages). Ordering information is given on any current masthead page.

(37) Loeb, S. J. Private communication.
(38) Prout, K.; Critchley, S. R.; Rees, G. V. *Acta Crystallogr., Sect. B* **1974**, *B30*, 2305.
(39) Daran, J. C.; Meunier, B.; Prout, K. *Acta Crystallogr., Sect. B* **1979**, *B35*, 1709.
(40) Baker, R. T.; Fultz, W. C.; Marder, T. B.; Williams, I. D. *Organometallics* **1990**, *9*, 2357.
(41) Rousseau, R.; Stephan, D. W. *Organometallics*, in press.
(42) Desper, J. M.; Gellman, S. H. *J. Am. Chem. Soc.* **1990**, *112*, 6732.